

Supporting Information

Materials and methods

10% buffered hydrofluoric acid (BHF, Transene Inc.), 30%(w/w) hydrogen peroxide (H_2O_2), concentrated hydrochloric acid (HCl), tungsten metal powder (W, Sigma Aldrich), platinum black (Pt-black, Sigma Aldrich), acetonitrile (CH_3CN , 99.8%, Sigma Aldrich), tetrabutylammonium hydrogen sulfate (TBA- HSO_4 , 97%, Sigma Aldrich), tetrabutylammonium tetrafluoroborate (TBA- BF_4 , 99%, Sigma Aldrich), silver nitrate (AgNO_3 , >99%, Sigma Aldrich) and tetrahydrofuran (THF, Sigma Aldrich) were used as received. 18 M Ω -cm resistivity water was obtained from a Barnstead Nanopure filtration system.

Si microwire growth

Boron-doped (0.001-0.005 Ω -cm resistivity), single-side polished, (111)-oriented p⁺-Si wafers (WRS Materials, San Jose, CA), obtained with a 300 nm-thick thermal oxide layer, were used as substrates for the growth of Si microwires¹. Photolithography was used to produce a pattern of 3 μm diameter holes on a 7 μm -pitch square lattice in a polymeric photoresist, and the oxide exposed by the holes in the photoresist was etched by immersion in BHF. 500 nm of high-purity Cu (99.9999%,) was then deposited onto the patterned wafer by thermal evaporation. The photoresist layer was then removed with acetone, leaving a patterned, oxide-confined, Cu catalyst layer on the wafer. Si microwires were grown by the vapor-liquid-solid chemical-vapor deposition process at 1000 °C at atmospheric pressure in flowing H_2 (500 sccm) and SiCl_4 (45 sccm), with small partial pressures of BCl_3 (1.3 sccm) as a p-type dopant. After microwire growth, the Cu catalyst was removed by immersing the substrates in an RCA2 etch (1:6:1 by volume HCl:H₂O:H₂O₂) for 20 min at 70 °C. This process produced patterned 1 μm diameter p-Si microwires on the degenerately doped p⁺-Si substrate.

To prepare the core-shell microwire structures, the substrates containing Si microwire arrays were etched in BHF for 20 s to remove native oxide on the microwire surface. A 125 nm layer of tin-doped indium oxide (ITO) was then deposited over the entire substrate by RF sputtering (90% In_2O_3 /10% SnO_2 target, Plasmaterials, Inc.). The ITO

layer produced a low-resistivity ohmic contact between the p-Si core and the n-type WO₃ shell layer, and was sufficiently transparent to allow light of energies below the WO₃ band gap to be absorbed in the Si².

Porous core-shell Si/ITO/WO₃ microwire synthesis

Conformal layers of WO₃ were then electrodeposited on the Si microwire/ITO substrates. To prepare the electrodeposition bath², a solution of peroxytungstic acid was prepared by slowly dissolving 4.6 g of W powder in 50 mL of 30%(w/w) H₂O₂(aq). After the powder had dissolved, the remaining H₂O₂ was decomposed with Pt black until the peroxide concentration was less than 3 mg mL⁻¹, as measured with peroxide testing strips. The solution was then filtered to remove the Pt black, and diluted with water and isopropanol until the final solution was 50 mM peroxytungstic acid in 65% water/35% isopropanol by volume.

Porous core-shell Si/ITO/WO₃ microwire arrays were prepared using electrodeposition of WO₃ in conjunction with sidewall-microsphere lithography. First, a Si microwire-array substrate with a sputtered ITO layer was connected to a wire by an alligator clip. The back and sides of the substrate were then painted with nail polish, to prevent deposition on these surfaces. A conformal base layer of WO₃ was then cathodically electrodeposited on the substrate. The electrodeposition was performed potentiostatically at -450 mV versus a Ag/AgCl reference electrode (CH Instruments), in a standard three-necked flask with a Pt wire as the counter electrode. The deposited tungsten oxide was solidified by annealing in air for 20 min at 200 °C. This base layer insulated the conductive ITO layer from making electrical contact with solution during photoelectrochemical characterization.

Solutions of polystyrene microspheres of a chosen diameter were prepared in Teflon vials by diluting 2.6%(w/w) stock aqueous solutions of microspheres (PolySciences Inc.) to 0.26% with water, to produce ~ 4 mL of diluted microsphere solution for each deposition. The microwire substrates were placed along the inside of the vial, and were oriented vertically with the full deposition area submerged in the microsphere solution. The vials were then placed in a temperature-controlled sand bath and covered to control the

surrounding airflow. The vials were submerged in the sand to the initial level of the microsphere solution and were held at $\sim 55\text{ }^{\circ}\text{C}$.

After the solvent had completely evaporated ($\sim 24\text{ hr}$), the film of microspheres was observed to have infiltrated the microwire substrate. Slight variations in the optical density were observed along the substrate in locations where temperature changes affected the evaporation rate of the solvent. Hence, the temperature was controlled ($55 \pm 3\text{ }^{\circ}\text{C}$) for all of the samples described herein. The substrates were removed from the vials and excess polystyrene material was scraped from the sides and the back of the substrate. The infilling polystyrene colloidal assembly was stabilized by sintering for 1 h at $98\text{ }^{\circ}\text{C}$, slightly below the glass-transition temperature of polystyrene³.

To prepare the porous shell layer, the microsphere-patterned substrate was electrically contacted to a wire by an alligator clip. The back and sides of the substrates were again painted with nail polish, to prevent deposition on these surfaces. WO_3 was potentiostatically electrodeposited, as described above, on the templated substrate until the desired charge density had been passed. The substrates were then annealed at $200\text{ }^{\circ}\text{C}$ in air for 20 min to solidify the electrodeposited film. After cooling to room temperature, the substrate was submerged overnight in THF to dissolve the polystyrene template. Finally, the substrates were annealed at $500\text{ }^{\circ}\text{C}$ for 2 h in air (ramp rate = $1\text{ }^{\circ}\text{C min}^{-1}$) to crystallize the WO_3 in the monoclinic phase. Plain core-shell Si/ITO/ WO_3 microwire arrays were prepared using nominally the same procedure, except that the production of the microsphere template was omitted from the process steps.

The total amount of electrodeposited WO_3 was controlled by limiting the total projected-areal charge passed during electrodeposition (-1.0 C cm^{-2} and -2.0 C cm^{-2}), not accounting for any additional surface area due to the microwires. For photoelectrochemical experiments, control electrodes of plain core-shell microwire arrays were prepared on substrates that had arrays of $15\text{ }\mu\text{m}$ -long p-Si microwires. WO_3 was electrodeposited onto these electrodes deposited in two steps, first with a base layer of -0.25 C cm^{-2} , and then with a second layer deposited until the desired total charge density (-0.75 C cm^{-2} or -1.75 C cm^{-2}) was reached. Scanning electron microscopy (SEM) images (Zeiss LEO 1550VP field-emission SEM) indicated that the diameters for these core-shell microwire

structures were $2.2(\pm 0.1) \mu\text{m}$ for -1.0 C cm^{-2} of total deposition charge density and $3.8(\pm 0.1) \mu\text{m}$ for -2.0 C cm^{-2} of total deposition charge density. To study the effect of patterning the WO_3 shell using sidewall microsphere lithography, core-shell microwire electrodes were prepared on $15 \mu\text{m}$ -long p-Si microwires with -1.0 C cm^{-2} of total charge density passed (-0.25 C cm^{-2} in the base layer, -0.75 C cm^{-2} in the porous layer), using microspheres having diameters of 350 nm, 500 nm, 750 nm, or 1000 nm. To minimize growth-to-growth variations in the Si microwires, all of the electrodes described herein were prepared from a single growth of Si microwire arrays.

Electrodes were prepared from microwire-array substrates by scratching Ga-In eutectic into the back of the substrate, and affixing the substrates to a tinned Cu wire with conductive Ag paint (SPI Supplies, Inc.). After the paint had dried, the wires were threaded through a glass tube and the substrate was sealed with epoxy (Hysol 9460), leaving only the microwire array exposed. The epoxy was cured overnight at room temperature and dried at $60 \text{ }^\circ\text{C}$ for 2 h. The area of each electrode was determined by scanning the electrode surface with a high-resolution (600dpi) scanner, followed by measurement of the active area with the ImageJ software package.

Photoelectrochemical characterization of core-shell Si/ITO/ WO_3 microwire electrodes

Photoelectrochemical current density vs. potential (J - E) data were obtained in CH_3CN solutions that had 100 mM TBA- HSO_4 as the supporting electrolyte. The electrochemical cell was a standard three-necked flask that had been modified to include a quartz window in the path of illumination. Under these solution conditions, HSO_4^- anions are photoanodically oxidized to $\text{S}_2\text{O}_8^{2-}$ at the WO_3 surface⁴. A platinum mesh was the counter electrode, and a Ag/Ag^+ reference electrode was prepared from a Ag wire in a solution of 10 mM AgNO_3 /10 mM TBA- BF_4 in CH_3CN . The light source was a 150 W Xe arc lamp (Oriel), mounted with a collimator and an Air-Mass 1.5 G (AM1.5G) filter.

Spectral response measurements were performed in the same electrolyte and cell conditions, but illumination was provided from a 150 W Xe arc lamp (Oriel) that was passed through a monochromator (Oriel Cornerstone 260, Newport Corp.) before striking the electrochemical cell. The electrode was held at a fixed potential (1.0 V vs. a Pt wire

poised at the Nernstian potential of the solution) and the photocurrent was measured with a Gamry Series G300 potentiostat. The illumination was focused to an area smaller than the active area of the photoelectrode ($<1 \text{ mm}^2$) and was chopped at a frequency of 1.0 Hz. A lock-in amplifier (SR830, Stanford Research Systems) was used to discriminate the chopped photocurrent from the dark current. The external quantum yield was calculated based on the wavelength-dependent photon flux as measured with a calibrated Si photodiode (UV-50, OSI Optoelectronics) at the sample position.

Simulations of Si/WO₃ core-shell absorption

Simulations of the light-absorption profiles in representative porous and plain core-shell structures were performed by finite-difference time-domain (FDTD) methods⁵ using the freely available software package MEEP⁶. Monochromatic simulations were performed by initially running the FDTD simulation until steady state was reached. The time-averaged absorption profile was then calculated from a single illumination period (1/frequency) of further simulation. The core and shell structures were assigned wavelength-dependent complex index of refraction values for Si⁷ and WO₃⁸, respectively, which were interpolated from published, spectroscopically determined data. Finite values for the extinction coefficient for wavelengths corresponding to energies near the band gap are not reported in the available data. However, spectroscopic measurements indicated that photocurrent was produced at these wavelengths (c.f., Figure 4e). To account for such behavior, the absorption values at these wavelengths were interpolated in the simulation between the last finite entry and a value of zero for wavelengths larger than 450 nm. The simulations were performed as a single core-shell microwire structure in a $7 \mu\text{m} \times 7 \mu\text{m}$ box (voxel size = 20 nm), with periodic boundary conditions in the x and y directions to represent an array of structures matching the geometry of the actual substrates used in the experiments. Perfectly matched absorber-layer (PML) boundaries were defined on the ends of the simulation box along the z-direction.

The core structure of the core-shell microwire was modeled as a $10 \mu\text{m}$ long Si microwire (radius = $0.5 \mu\text{m}$) with a $0.1 \mu\text{m}$ thick WO₃ base layer. The shell structure was modeled as a cylinder with spherical voids of a single diameter to represent the pores generated by the templating microspheres. Because SEM images indicated that the microsphere

assemblies were close-packed and highly periodic, the spherical voids were arranged in a face-centered cubic lattice, in accord with the behavior of artificial opals grown by evaporative self-assembly⁹. Spheres that overlapped with the core structure were omitted from the lattice, so the core structure was unchanged by the presence of voids. The radius of the cylinder that represented the shell structure was chosen so that the volume of the porous structure was equal to the volume of a plain core-shell microwire having a radius of $1.3 \mu\text{m}$. This radius was nearly $2 \mu\text{m}$ for all chosen diameters of the microspheres, except for the 750 nm porous core-shell microwire. Compared to spheres of other diameters, the omission condition of the definition of the lattice of void spheres in the simulation resulted in a longer distance of closest approach to the microwire core for 750 nm diameter spheres. This condition resulted in a larger volume of untemplated WO_3 near the center of the 750 nm case compared to the other porous structures, and an overall smaller diameter for the cylinder representing the shell structure required to satisfy the equal volume constraint of the simulation geometry. Table SI.1 contains a table of the chosen radii and volumes for each geometry.

| Template sphere diameter | radius(um) | volume(um ³) |
|--------------------------|------------|--------------------------|
| None (equal volume case) | 1.3 | 61.58 |
| None (equal radius case) | 2.065 | 175.7 |
| 350nm | 2.079 | 61.88 |
| 500nm | 2.063 | 61.58 |
| 750nm | 1.837 | 61.13 |
| 1000nm | 2.064 | 61.63 |

Table SI.1 - Chosen radius and calculated volume for plain and porous core-shell structures used in FDTD simulations.

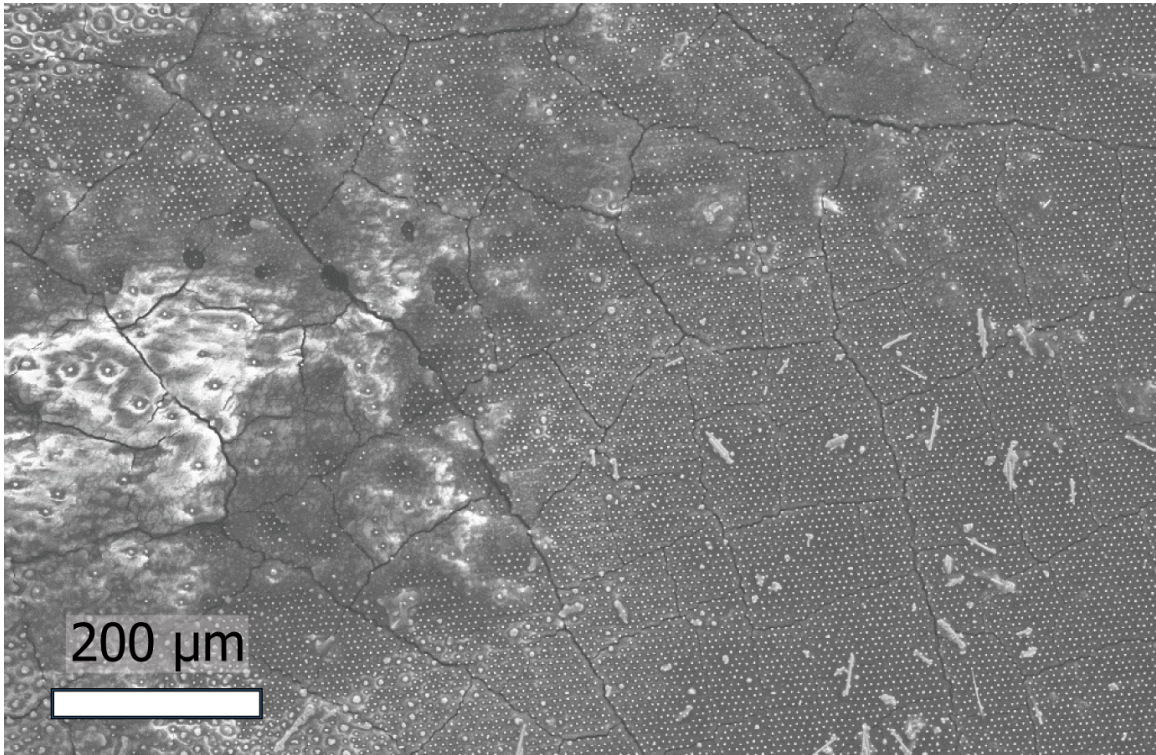


Figure SI.1 - SEM image of a Si microwire array patterned with a continuous assembly of polystyrene microspheres. The regularly ordered white dots in the image are the tips of the microwires near the top of the template. Microwire substrates can be patterned with this uniformity over all of the substrates sizes tested here, up to 2cm².

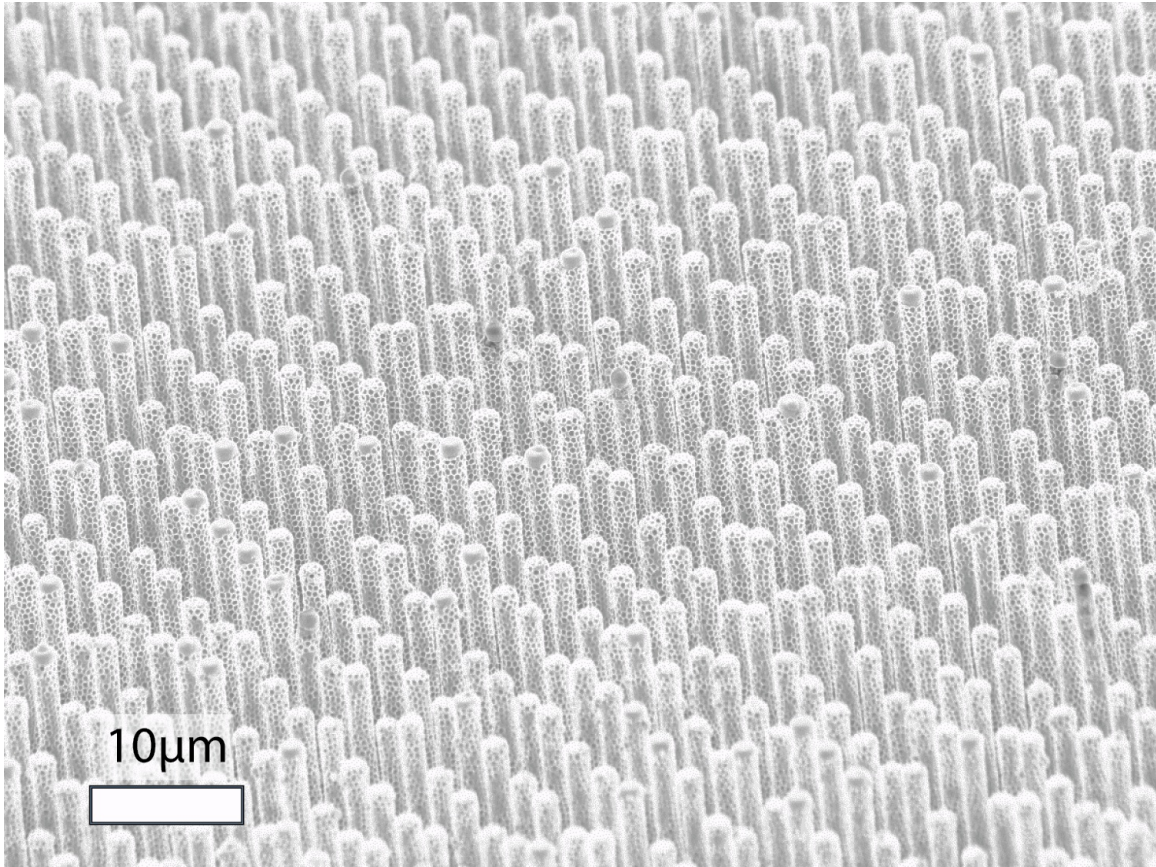


Figure SI.2 - An SEM image of microsphere templated porosity on a Si/ITO/WO₃ microwire array. This image represents the maximum field of view of the SEM, but patterning with this fidelity was observed throughout the entire sample (1cm²).

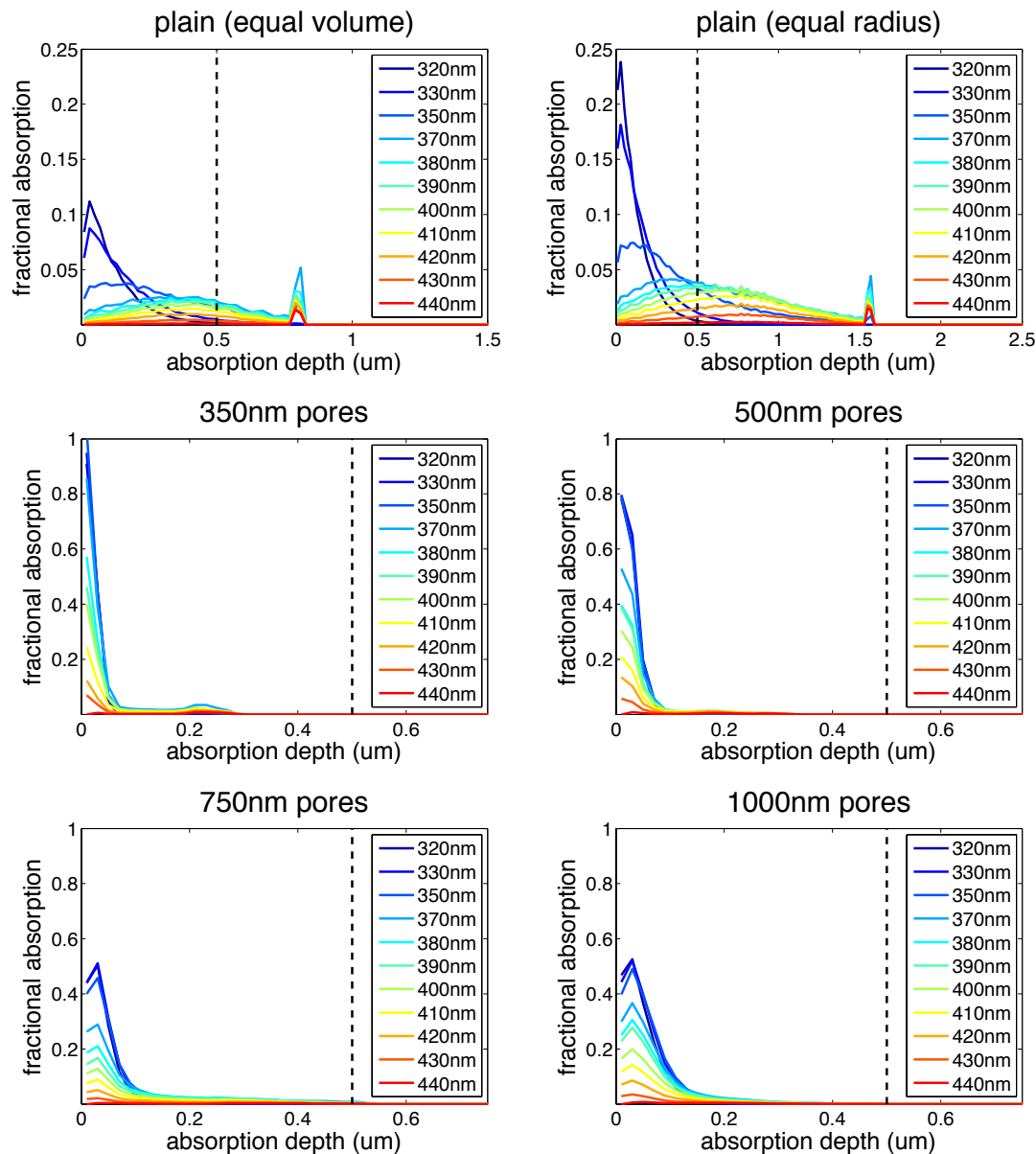


Figure SI.3 - Integrated depth profiles of fractional absorption in the WO_3 shell of a Si/WO_3 core-shell microwire as calculated from FDTD simulations. For plain core-shell equal volume and equal radius electrodes, a significant fraction of illumination is absorbed at depths much larger than the minority carrier diffusion length ($L_p=500\text{nm}$, dashed black line). In the porous core-shell structures, almost all of the absorption occurs at depths much shallower than L_p due to the small feature size of the inverse opal structure.

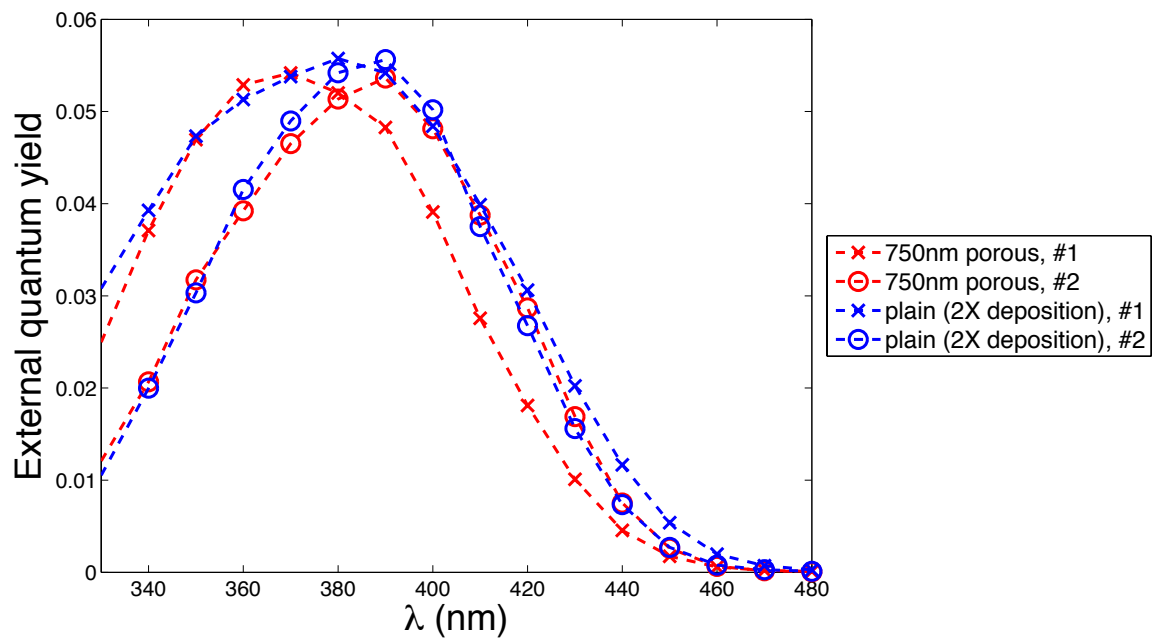


Figure SI.4 - External quantum yield measurements for independently prepared, p-Si/ITO/WO₃ core-shell electrodes for the (red) -0.25/-0.75 C cm⁻², 750nm porous core-shell electrodes and (blue) -0.25/-1.75 C cm⁻² plain core-shell electrodes.

References:

1. Kelzenberg, M. D.; Boettcher, S. W.; Petykiewicz, J. A.; Turner-Evans, D. B.; Putnam, M. C.; Warren, E. L.; Spurgeon, J. M.; Briggs, R. M.; Lewis, N. S.; Atwater, H. A. *Nat Mater* 2010, 9, (3), 239-244.
2. Coridan, R. H.; Shaner, M.; Wiggenhorn, C.; Brunshwig, B. S.; Lewis, N. S. *J. Phys. Chem. C* 2013, 117, (14), 6949-6957.
3. Wunderlich, B.; Bodily, D. M.; Kaplan, M. H. *Journal of Applied Physics* 1964, 35, (1), 95-102.
4. Mi, Q.; Coridan, R. H.; Brunshwig, B. S.; Gray, H. B.; Lewis, N. S. *Energy Environ. Sci.* 2013, 6, (9), 2646-2653.
5. Taflove, A.; Hagness, S. C., *Computational Electrodynamics: The Finite-Difference Time-Domain Method*. 3rd ed.; Artech House: 2005.
6. Oskooi, A. F.; Roundy, D.; Ibanescu, M.; Bermel, P.; Joannopoulos, J. D.; Johnson, S. G. *Computer Physics Communications* 2010, 181, (3), 687-702.
7. Aspnes, D. E.; Studna, A. A. *Phys. Rev. B* 1983, 27, (2), 985-1009.
8. von Rottkay, K.; Rubin, M.; Wen, S. J. *Thin Solid Films* 1997, 306, (1), 10-16.
9. Míguez, H.; López, C.; Meseguer, F.; Blanco, A.; Vázquez, L.; Mayoral, R.; Ocaña, M.; Fornés, V.; Mifsud, A. *Applied Physics Letters* 1997, 71, (9).